Macrophages promote aberrant DNA repair in multiple myeloma via the CXCL5/8-CXCR2 axis

Mengmeng Dong;[1,2*] Donghua He,[1*] Jinna Zhang,[1,2*] Haimeng Yan,[1] Haoguang Chen,[1] Enfan Zhang,[1] Yili Feng,[2,3] Jingsong He,[1] Xi Huang,[1] Guoqiao Chen,[2,3] Xiuna Sun,[2,3] Fei Cheng,[4] Huiyao Gu,[1] Huanping Wang,[1] Anyong Xie[2,3] and Zhen Cai[1,5]

[1]Bone Marrow Transplantation Center, The First Affiliated Hospital, School of Medicine, Zhejiang University, Hangzhou Zhejiang; [2]Institute of Translational Medicine, Zhejiang University School of Medicine and Zhejiang University Cancer Center, Hangzhou, Zhejiang; [3]Innovation Center for Minimally Invasive Technique and Device, Department of General Surgery, Sir Run Run Shaw Hospital, Zhejiang University School of Medicine, Hangzhou, Zhejiang; [4]Pathology Department, The First Affiliated Hospital, School of Medicine, Zhejiang University, Hangzhou, Zhejiang and [5]Institute of Hematology, Zhejiang University, Hangzhou, Zhejiang, China

MD, DH and JZ contributed equally as first authors.

Correspondence: Z. Cai
caiz@zju.edu.cn.

A. Xie
anyongxie@zju.edu.cn

Received: January 7, 2025.
Accepted: June 18, 2025.
Early view: June 26, 2025.

https://doi.org/10.3324/haematol.2025.287312

Supplemental information

Title

Macrophages promote aberrant DNA repair in multiple myeloma via the CXCL5/CXCR2 axis

Authors

Mengmeng Dong[1,2]*, Donghua He [1]*, Jinna Zhang[1,2]*, Haimeng Yan[1], Haoguang Chen [1], Enfan Zhang[1], Yili Feng[2,3], Jingsong He[1], Xi Huang[1], Guoqiao Chen[2,3], Xiuna Sun[2,3], Fei Cheng[4], Huiyao Gu[1], Huanping Wang[1], Anyong Xie[2,3#] and Zhen Cai[1,5#]

This PDF file includes:

1) Supplementary Methods
2) Supplementary References
3) Supplementary Figures S1-S11
4) Supplementary Tables S1-S6

1) Supplementary Methods

1. Cells

MM cell lines ARP-1, OPM2, MM.1S, and CAG were obtained from Shanghai Cell Bank. Freshly isolated $CD138^+$ MM cells were purified by positive selection using CD138 microbeads (Miltenyi Biotech, San Diego, CA, USA). All MM cells were cultured with fresh RPMI 1640 medium (Corning, USA) containing 10% FBS (Gibco, USA) at 37°C in an incubator with 5% CO_2 and saturated humidity. U2OS cells carrying the SCR reporter (an HR reporting system) [1] and U2OS cells carrying the vGEJ reporter (an NHEJ reporting system) [2] were used as described previously.[1, 2] These cells were cultured in high-sugar DMEM containing 10% FBS (Biological Industries, Israel) in a 37°C and 5% CO_2 incubator. HEK293T cells were obtained from Shanghai Cell Bank. The culture method was similar to that used for U2OS cells.

MΦs were obtained by peripheral blood mononuclear cells from heathy donors as previously described.[3, 4] In short, mononuclear cells were seeded in a 6-well plate with serum-free RPMI 1640 and placed in an incubator for 1–2 hours. When more than 90% of the cells adhered to the

wall, we aspirated the medium (while discarding the suspended cells) and added fresh complete RPMI 1640 medium containing 10 ng/ml M-CSF (Novus Biologicals, USA) to the adherent cells. The medium was changed every other day until the cells were cultured for 5–7 days to mature. M-CSF-induced MΦs were then harvested. Except for the MΦs in Figure 8E, which induced from different patients (including healthy donors and different MM patients), all others were from healthy donors.

MM cells (suspension cells) were inoculated at a density of 0.5–1.0 × 10^6 cells/ml with MΦs cultured 5–7 days previously, treated according to the experimental requirements, and incubated for a certain period of time (for 1 hour–48 hours). MM cells were purified by positive selection using CD138 microbeads (Miltenyi Biotech, San Diego, CA, USA).

T cells, NK cells and Neutrophils were isolated from peripheral blood, by EasySepm Human CD3 Positive Selection Kit II (Catalog #17851), RosetteSep™ Human NK Cell Enrichment Cocktail (Cat#15065) and EasySep Direct Hu Neutro lso Kit (Stem Cell, Cat#19666), respectively, sorted according to the product manuals. The isolated T and NK cells were incultured in RPMI1640 with 10% FBS and 10 ng/ml IL-2, while Neutrophils cells in RPMI 1640 medium containing 10% FBS.

The stromal cells were induced from patints' bone marrow, by the method described in the previous publication[5]. In brief, the mononuclear cells were seeded in a 6-well plate with 10% FBS DMEM, and the medium was changed every other day until adherent cells were spindle shaped and covered with culture plates.

2. Western blot

Cultured MM cells were collected, lysed with protease lysis buffer (RIPA) (Applygen, China) containing protease and phosphatase inhibitors (Thermo, USA), and centrifuged at 4°C at 12,000 rpm for 15–20 min. A Bio-Rad Protein Assay was used to detect the protein concentrations, obtained from the supernatant. The prestained protein molecular weight standard marker (GeneStar, China, and Fermentas, USA) and the same amount of protein samples (10–30 μl) were added to the wells of the appropriate SDS-PAGE precast gel (Invitrogen, USA). Electrophoresis apparatus (Bio-Rad, USA), PVDF membrane (Millipore, USA) with a protein vertical transfer instrument (Bio-Rad, USA) were applied. The PVDF membrane was incubated successively with specific antibodies against relevant proteins and secondary antibodies. Finally, a

chemiluminescence imaging instrument (Bio-Rad, USA) was used for image acquisition.

3. Reverse transcription quantitative PCR (RT-qPCR)

Total RNA was isolated from MM cells or MΦs by using the TRIzol reagent (Takara, Japan). A total of 1000 ng isolated RNA was reverse transcribed into complementary DNAs according to the HiScript II Q RT SuperMix for real-time quantitative PCR (qPCR) with a qPCR kit (Vazyme, China). RT-qPCR assays were carried out using a CFX-96 RT-PCR detection system (Bio-Rad) with SYBR Green qPCR master mix (Vazyme, China) following the manufacturer's protocol, and each sample was performed in triplicate. Relative mRNA content was normalized to Ubiquitin B (UBB) and β-actin (ACTB) content for MM cells and MΦs respectively. RT-qPCR data were presented as fold differences by the 2-ΔΔCt method. The primer sequences for qPCR are provided in Table S1.

4. Enzyme-linked immunosorbent assay (ELISA)

The supernatant concentration of CXCL5 or CXCL8 secreted by MΦs or MM cells was determined by ELISA kits including Human CXCL5 ELISA kit (Cat#RK00268) and Human CXCL8 ELISA kit (Cat#RK00011) from Abclonal (Wuhan, China), according to the manufacture's protocols.

5. Flow cytometry

Flow cytometric detection of the expression of CD80, CD86, CD163, and CD206 on the surface of the MΦs was performed as previously decribed (references). For flow cytometric detection of cell apoptosis, cells were resuspended and washed twice with PBS and the tested samples were prepared with an Annexin V-PI Apoptosis Detection Kit (Dojindo, Kumamoto, Japan). For flow cytometric measurement of HEK293T transfection efficiency or U2OS-HR/NHEJ levels, HEK293T cells transfected with GFP plasmids or U2OS-HR/NHEJ cells transfected for 72 hours were washed with PBS twice and 200 μl of trypsin were added to digest the cells at 37°C for 5 min. Cells were analyzed with a flow cytometer (Bio-Rad and Beckman, USA), and the data were determined with FlowJo 10.0 software.

6. Immunofluorescence and immunohistochemistry

Immunofluorescence analysis: pre-prepared MM cells were added to each well of the 6-well plates at a density of 0.1×10^6–1.0×10^6 cells/well. The plate was centrifuged at 1500 rpm for 5 min and placed in the incubator overnight. After gentle washing 3 times with PBS, 4%

paraformaldehyde was added to fix the cells. After 3 washes, pre-prepared 5% BSA solution, primary antibody and fluorescent secondary antibody were added. After another gentle wash, sections were stained with DAPI (Servicebio, China). Finally, the slides were mounted with anti-fluorescence quenching mounting tablets (Servicebio, China) and stored at 4°C in the dark. Cellular immunofluorescence was initially observed under an inverted fluorescence microscope (Zeiss, Germany). Images were acquired on a high-content cell imaging system (PerkinElmer, USA), by which the number of cells was determined, and the number of foci and fluorescence intensity were calculated. The data were sorted and analyzed with Excel and GraphPad 7.0.

Immunohistochemistry: paraffin sections of bone marrow tissues were obtained from MM patients. After paraffin sections were deparaffinized, slides underwent antigen retrieval and were blocked for endogenous peroxidase, and 3% BSA was dripped onto the samples and sealed at room temperature for 30 min. Then, blocking solution was removed, the sections flat was placed in a wet box, and diluted primary antibody was added and incubated overnight at 4°C. The samples were washed with PBS. The sections were dried, and the corresponding secondary antibody was dropped. After further washing, the slices were dried. DAB chromogenic solution (Servicebio, China) was added to the tissue circles, and microscope observation showed a brown-yellow color, which indicated positivity. After counterstaining the nuclei, dehydration, and mounting with neutral gum, the images were collected and analyzed under a microscope. We chose 3 fields of view (200 ×) for each slice of each sample. The uniform positive standard was selected and the images were analyzed by Image-Pro Plus 6.0 software to obtain the integrated optical density (IOD) value.

7. Reagents

Antibodies used for Western blot, immunofluorescence, and flow cytometry include anti-GAPDH (Abcam, ab181602), anti-CXCR2 (Abcam, ab65968), anti-rabbit IgG (H+L), biotinylated antibody (CST, 14708), anti-mouse IgG (H+L), biotinylated antibody (CST, 14709), γH2AX (CST, 9718S), APC anti-human CD80, FITC anti-human CD86, PerCP/Cy5.5 anti-human CD163, and PE anti-human CD206 (Biolegend, USA). Human IL-8/CXCL8 neutralizing antibody (Cat#MAB208), human CXCL5/ENA-78 neutralizing antibody (Cat#MAB654) and the corresponding isotype control antibody from R&D Systems (Minneapolis, MN, USA) were dissolved in sterile PBS at 0.5 mg/mL. CXCR2 antagonist 8 (Cat#HY-147392)

from MedChemExpress was dissolved in DMSO.

Bortezomib (Cat#S1013), melphalan (Cat#S8266), dexamethasone (Cat#S1322) and bleomycin (Cat#S1214) were purchased from Selleck, USA and dissolved in DMSO.

Recombinant human CXCL5 protein (Cat#254-XB), recombinant human CXCL8 protein (Cat#208-IL), recombinant human CXCL3 protein (Cat#277-GG) and recombinant human CXCL6 protein (Cat#333-GC) from R&D Systems (Minneapolis, MN, USA) were dissolved in sterile PBS at 100 μg/mL containing 0.1% bovine serum albumin.

8. Comet assay

The experiments were carried out according to the instructions of the Comet Assay Kit (Trevigen, 4250-050-K). Briefly, LMAgarose was added to a 1.5 ml EP tube at 37°C and cells were mixed at 1×10^5/ml for testing. The comet slides were preheated to 37°C in advance, and the cell-LMAgarose mixture was pipetted on the sample area of the slides. The slides were kept at 4°C in the dark for 10 min and then immersed in 4°C precooled lysis solution in dark for 30–60 min. Excess lysate was removed and the slides were placed in freshly prepared alkaline solution in dark, following in the alkaline unwinding solution electrophoresed at a constant voltage of 21 V for approximately 30 min in a horizontal electrophoresis apparatus at 4°C in dark. After the comet slides being soaked in ddH_2O for 5 min and incubated in 70% ethanol for 5 min, comet slides were removed and dried, diluted SYBR® GOLD Nucleic Acid Gel Stain (Thermo, USA) was pipetted into the gel rings on the dried comet slides. Slides were placed under a fluorescence microscope for observation, with a maximum excitation/emission wavelength of 496 nm/522 nm, and collected the images. CASP_1.2.3 software was applied to analyze the comet pictures and calculate the proportions of damaged DNA.

9. 3’ 10X Single-cell RNA sequencing

The samples were from bone marrow of NDMM and RRMM. The therapeutic history of the RRMM patients were not completely consistent (P1: Bortezomib, Doxorubicin, Cyclophosphamide, Dexamethasone, Lenalidomide, Isazomib; P2: Bortezomib, Cyclophosphamide, Dexamethasone, Lenalidomide, Xidabenzamide, Isazomib, Pomalidomide; P3: Bortezomib, Dexamethasone, Daretomumab). Single-cell lysates of bone marrow from myeloma patients were loaded onto 10x Chromium to capture 5000 single cells, according to the

manufacturer’s instructions for the 10 × Genomics Chromium Single-Cell 3’ kit (V3). The following cDNA amplification and library construction steps were performed according to the standard protocol. Libraries were sequenced on an Illumina NovaSeq 6000 sequencing system (paired-end multiplexing run, 150bp) by LC-Bio Technology co.ltd., (HangZhou, China) at a minimum depth of 20,000 reads per cell.

Sequencing results were demultiplexed and converted to FASTQ format using Illumina bcl2fastq software (version2.20). All expression matrices from different studies were obtained from CellRanger Version 6.1.2. GRCh38 served as the reference genome and was downloaded from https://cf.10xgenomics.com/supp/cell-exp/refdata-gex-GRCh38-2020-A.tar.gz.

Seurat 4.3.0 and scanpy 1.7.2 were used for reading, filtrating, clustering, and visualizing (9, 10). Cells whose detected genes less than 200 or a mitochondrial gene percent higher than 10% were filtered out. R package harmony 0.1.1 was used to remove the batch effect.

10. Transient siRNA transfection

SiRNA transfection was performed using a scrambled nontargeting siRNA (siCon) and siRNAs specifically targeting CXCL5 (siCXCL5) or CXCL8 (siCXCL8), which were procured from Tsingke Biotechnology, China. Transfection of siRNAs into cells was conducted following the manufacturer's protocol. Briefly, attached MΦs were incubated in Opti-MEM (Gibco, USA) with a complex of either CXCL5 or CXCL8 siRNA, or the control siRNA, along with Lipofectamine RNAiMAX transfection reagent (Invitrogen, CA, USA) for a duration of 24 hours. Subsequently, the medium containing the siRNA transfection reagent complexes was aspirated and replaced with RPMI-1640 medium supplemented with 10% FBS and 10 ng/mL M-CSF for an additional 24 hours prior to conducting functional studies. The sequence of siRNA is as follows:

siCXCL5-1 5′- GAUCAGUAAUCUGCAAGUGUUTT -3′;

siCXCL5-2 5′- CGGGAAGGAAAUUUGUCUUGATT -3′;

siCXCL8-1 5′-GCUUUCUGAUGGAAGAGAGTT-3′;

siCXCL8-2 5′-CAAAGAACUGAGAGUGAUUTT-3′.

11. Plasmids and lentivirus

Expression plasmids for gRNAs were constructed in the U6sgDNA vectors as described previously.[6] The pcDNA3β-based expression vectors for I-SceI and GFP were described

previously.[2] We purchased the Cas9 plasmid pX330 originally from Addgene (catalog number 42230). gRNA target sequences are provided in Tables S1. Newly constructed plasmids were confirmed by Sanger sequencing.

The lentiCRISPRv2 lentiviral vector plasmids psPAX2 and PMD2. G lentiviral packaging plasmids were donated by Professor Huang He, Zhejiang University School of Medicine. The negative control lentivirus LV-sgRNA-CON244 (vector U6-sgRNA-SV40-EGFP), the Cas9 lentivirus LV-Cas9-puro (7768-1) (Ubi-3FLAG-Cas9-SV40-puromycin, LVCON249), LV-AAVS1-sgRNA (04799-1) lentivirus (contains two gRNAs at the AAVS1 locus with sequences of GGGCCACTAGGGACAGGAT and AGACCCAATATCAGGAGACT), and LV-HBB-sgRNA (04800-1) lentivirus (contains two gRNAs at the HBB locus with sequences of GGTATCAAGGTTACAAGAC and GTAACGGCAGACTTCTCCTC) were all purchased from Shanghai GeneChem Co., Ltd.

12. Genomic DNA extraction, PCR amplification, and Illumina deep sequencing

Cell genomic DNA extraction: Cells were collected, washed twice with PBS, centrifuged, and the supernatant was collected for later use. According to the instructions of the Multisource Genomic Miniprep DNA Kit (Axygen, USA), genomic DNA was extracted, and the DNA concentration was detected on a NanoDrop 2000 system and stored at -20°C for later use.

Specific new fragments of gRNAs targeting AAVS.1 and HBB were obtained by annealing according to the primers in Table S1 and then ligated into the U6sgDNA plasmid. The target gene was amplified by PCR with primers from Table S1. PCR products were purified using a gel extraction kit (Axygen, USA). Specific fragments of gRNA targeting IgH and CCND1 were obtained by annealing according to the primers in Table S1 and then ligated into the lentiCRISPRv2 plasmid. The detection of chromosomal translocation was performed with primers from Table S1 for PCR amplification.

Second-generation sequencing: The VAHTSTM Universal DNA Library Prep Kit for Illumina® (Vazyme, China) was applied to construct libraries for the above PCR products. PCR products from two to four different genomic target sites were mixed, end-repaired, adenylated at 3′ ends, ligated with adapters, purified, and amplified by the second round of PCR to combine the P7 and P5 Illumina adapters and a unique 8-mer barcode sequence according to the manufacturer's protocols. NGS was performed on an Illumina HiSeq system at Veritas Genetics

Asia, Inc. (Hangzhou). Sequences were analyzed to identify edited events with different indels at repair junctions by DBS-Aligner as described previously.[7]

NGS for translocation fragments detecting. To obtain more effective translocation fragment reads, translocation der 11 and β-actin fragments were mixed at a ratio of 8:1.

13. Transfection

HEK293T cells cultured in flasks were washed twice with PBS, digested with trypsin at 37°C for 2 min, and neutralized by adding complete medium. We seeded cells in a 24-well plate at 1.2×10^5 cells/well, and when the HEK293T cell confluence was approximately 70%, the next day, we combined Cas9 and the paired gRNA plasmids at a mass ratio of 2:1:1 using Lipofectamine 2000 transfection reagent (Invitrogen, USA) for transfection. Then, we changed the medium after 24 hours and cultured the transfected cells for 48–72 hours as needed.

14. HR and NHEJ reporter assays

We inoculated well-grown U2OS-HR/NHEJ cells in a 6-well plate at a concentration of 5×10^5 cells/well. When the confluence reached approximately 80%, gRNAs and Cas9 plasmids or I-SceI plasmids were transfected into the cells, and medium was changed after 8 hours with 2 ml of fresh complete DMEM high-glucose medium. Cells were resuspended, 1 ml of the cell suspension was pipetted into a new 6-well plate (control group), and another 1 ml was added to the Transwell compartments with mature MΦs (the MΦs group). After 72 hours, GFP (for NHEJ), GFP and RFP (for HR) were measured with a Beckman CytoFLEX flow cytometer. CytExpert software was used to analyze the cell HR and NHEJ repair levels.

15. Statistical analysis

The measurement data are expressed as mean ± standard deviation (mean ± SD). Unpaired two-tailed t-test, paired two-tailed t-tests, χ^2 tests and Mann–Whitney U tests were used to compare the two groups of samples. For details, refer to the figure legends. $P < 0.05$ was regarded as statistically significant, and $0.01 \leq P < 0.05$, $0.001 \leq P < 0.01$, and $P < 0.001$ were regarded as *, **, and ***, respectively. Otherwise, the differences were regarded as not significant (NS).

FlowJo10.0 and CytExpert software was used to analyze the flow cytometric data, and comet image analysis was performed with CASP_1.2.3 software. SPSS 24.0 and GraphPad 7.0 were used for data statistics.

The reading software, jointly developed with Hangzhou Shurui Technology Co., Ltd., read

and classified the second-generation sequencing data.

2) Supplementary References

1. Rass E, Chandramouly G, Zha S, Alt FW, Xie A. Ataxia telangiectasia mutated (ATM) is dispensable for endonuclease I-SceI-induced homologous recombination in mouse embryonic stem cells. The Journal of biological chemistry. 2013;288(10):7086-7095.

2. Xie A, Kwok A, Scully R. Role of mammalian Mre11 in classical and alternative nonhomologous end joining. Nature structural & molecular biology. 2009;16(8):814-818.

3. Zheng Y, Cai Z, Wang S, et al. Macrophages are an abundant component of myeloma microenvironment and protect myeloma cells from chemotherapy drug-induced apoptosis. Blood. 2009;114(17):3625-3628.

4. Yan H, Dong M, Liu X, et al. Multiple myeloma cell-derived IL-32gamma increases the immunosuppressive function of macrophages by promoting indoleamine 2,3-dioxygenase (IDO) expression. Cancer letters. 2019;446(38-48.

5. Damerau A, Pfeiffenberger M, Weber MC, et al. A Human Osteochondral Tissue Model Mimicking Cytokine-Induced Key Features of Arthritis In Vitro. International journal of molecular sciences. 2020;22(1):

6. Feng YL, Xiang JF, Liu SC, et al. H2AX facilitates classical non-homologous end joining at the expense of limited nucleotide loss at repair junctions. Nucleic Acids Res. 2017;45(18):10614-10633.

7. Guo T, Feng YL, Xiao JJ, et al. Harnessing accurate non-homologous end joining for efficient precise deletion in CRISPR/Cas9-mediated genome editing. Genome Biol. 2018;19(1):170.

8. Dellino GI, Palluzzi F, Chiariello AM, et al. Release of paused RNA polymerase II at specific loci favors DNA double-strand-break formation and promotes cancer translocations. Nat Genet. 2019;51(6):1011-1023.

9. Panchakshari RA, Zhang X, Kumar V, et al. DNA double-strand break response factors influence end-joining features of IgH class switch and general translocation junctions. Proc Natl Acad Sci U S A. 2018;115(4):762-767.

3) **Supplementary Figures S1-S11**

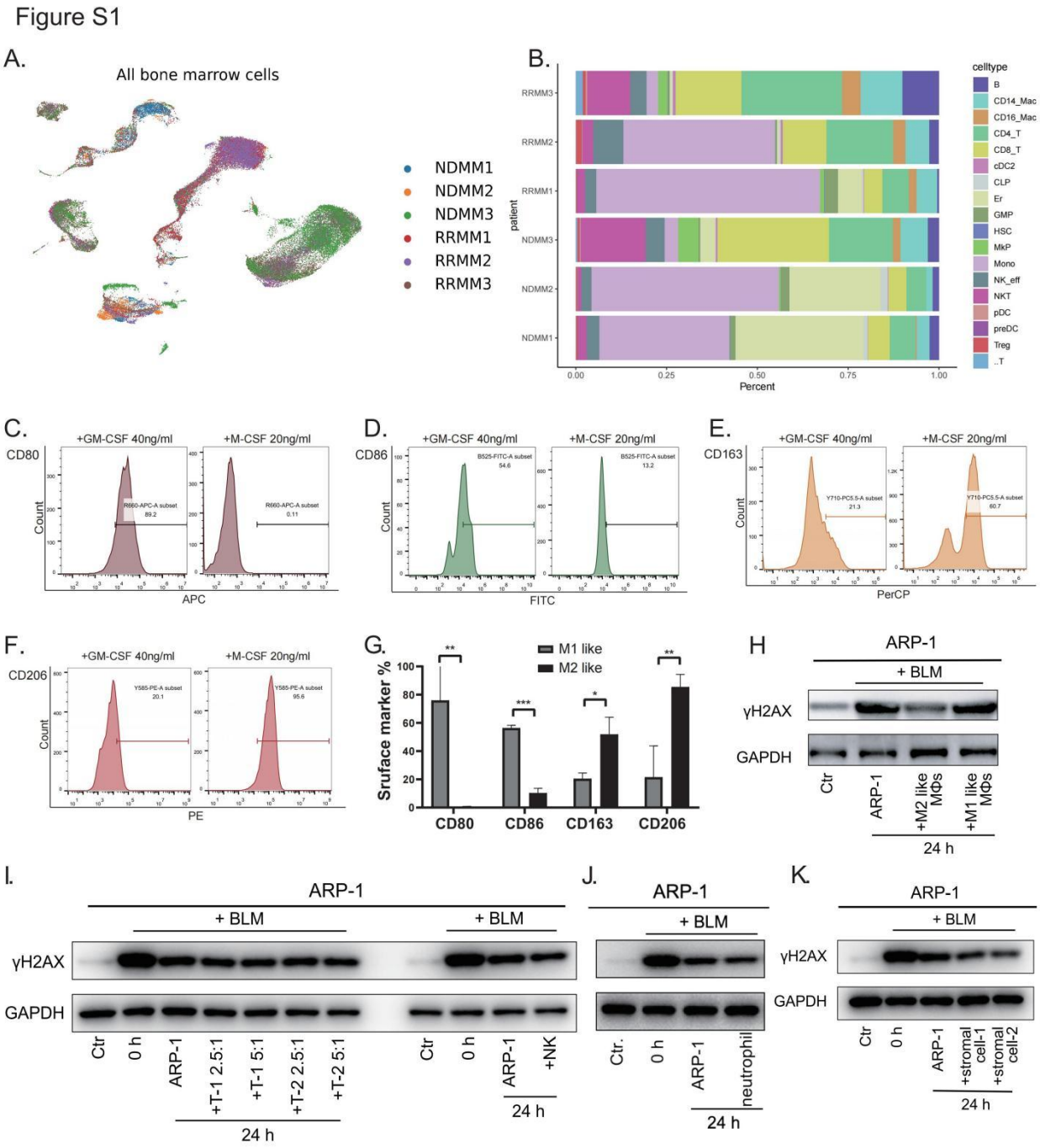

Figure S1, related to Figure 1. Induced MΦs were M2 like and promoted DNA repair of ARP-1 cells.

A. Single-cell RNA-seq sequencing of bone marrow cells from MM patients recognized the macrophages. Three newly diagnosed MM (NDMM) and 3 relapsed and refractory MM (RRMM) were involved. Batch effect removing result was shown.

B. Distribution of different non tumor cells in NDMM and RRMM bone marrow.

C-F. Flow cytometry detected CD80 (C), CD86 (D), CD163 (E) and CD206 (F) in MΦs.

G. The expression of CD80 and CD86 in the induced MΦs (M2 like) was low, while the expression of CD163 and CD206 was high (unpaired two-tailed t-test).

H. Western blot showed induced MΦs (M2 like) promoted DNA repair of ARP-1 cells.

I-K. Western blot showed isolated T, NK cells (I) and neutrophils (J) had no significant effect on DNA repair of ARP-1 cell, while cultured stromal cells had subtlely improve DNA repair of ARP-1 cell (K).

Figure S2

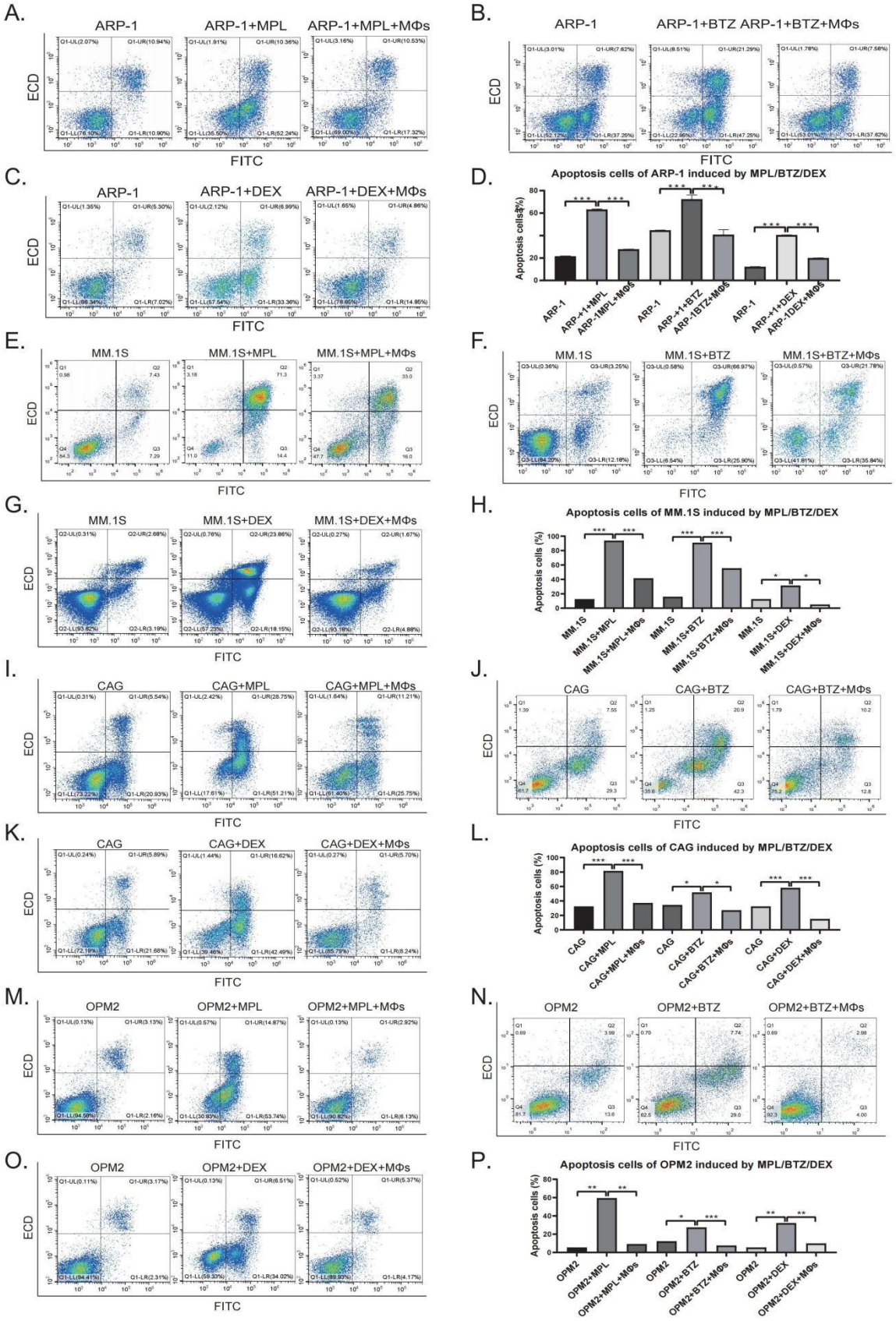

Figure S2, related to Figure 1. MΦs protected MM cells from chemotherapeutic agent-induced

apoptosis. Flow cytometry showed that MΦs reduced the apoptosis of ARP-1 (A-D), MM.1S (E-H), CAG (I-L) and OPM2 (M-P) cells induced by MPL, BTZ and DEX (unpaired two-tailed t-test, $0.01 \leq P < 0.05$, $0.001 \leq P < 0.01$, and $P < 0.001$ were regarded as *, **, and ***, respectively).

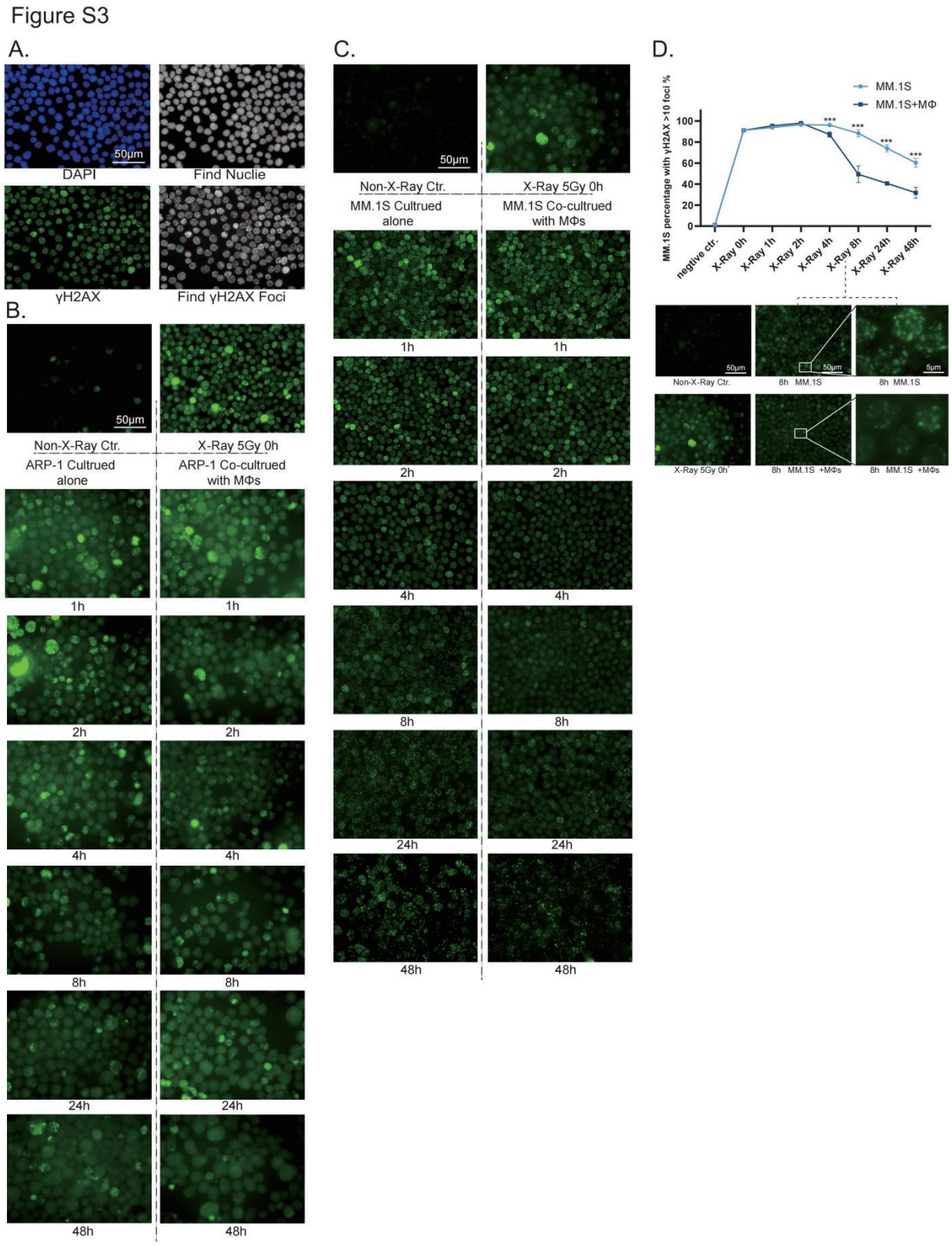

Figure S3, related to Figure 1. Immunofluorescence showed γH2AX foci in MM cells (ARP-1 and MM.1S) decreased faster in the MΦs cocultured group.

A. Images showing the high-content cell imaging system to find nuclei and γH2AX foci.

B. Immunofluorescence images showed γH2AX foci in ARP-1 cells with DNA-inducing X-ray irradiation for 5 Gy with or without MΦs.

C. An immunofluorescence experiment was performed for γH2AX foci in MM.1S cells with DNA-inducing X-ray irradiation at 5 Gy with or without MΦs.

D. A high-content imaging system was used to automatically capture the nuclei and γH2AX foci and count the number of MM.1S cells with more than 7 γH2AX foci (marked as $\gamma H2AX^{+}$) (unpaired two-tailed t-test).

Figure S4

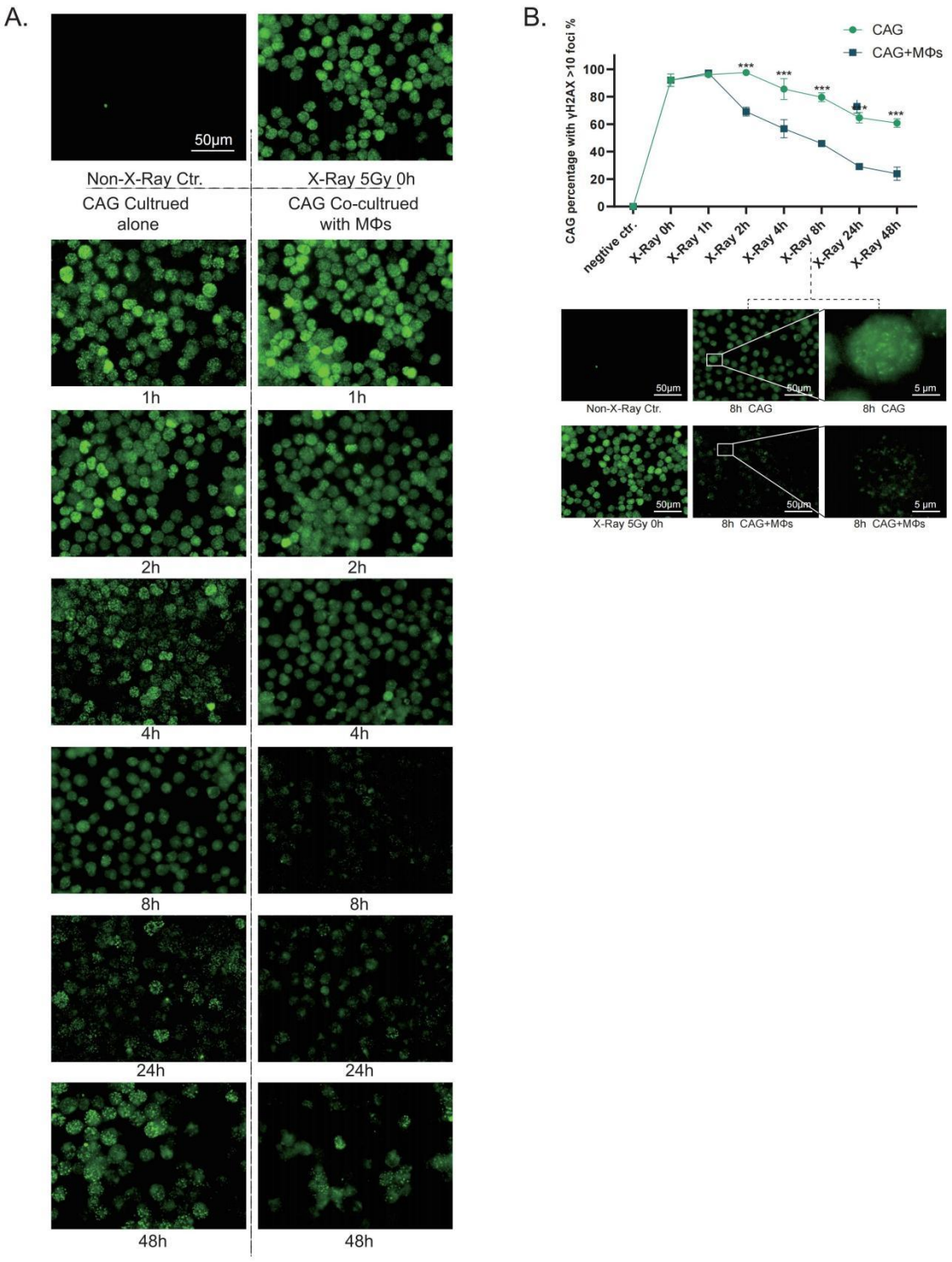

Figure S4, related to Figure 1. Immunofluorescence showed γH2AX foci in MM cells (CAG) decreased faster in the MΦs cocultured group.

A. An immunofluorescence experiment was performed for γH2AX foci in CAG cells with DNA-inducing X-ray irradiation at 5 Gy with or without MΦs.

B. A high-content imaging system was used to automatically capture the nuclei and γH2AX foci and count the number of MM.1S cells with more than 7 γH2AX foci (marked as $\gamma H2AX^{+}$) (unpaired two-tailed t-test).

Figure S5

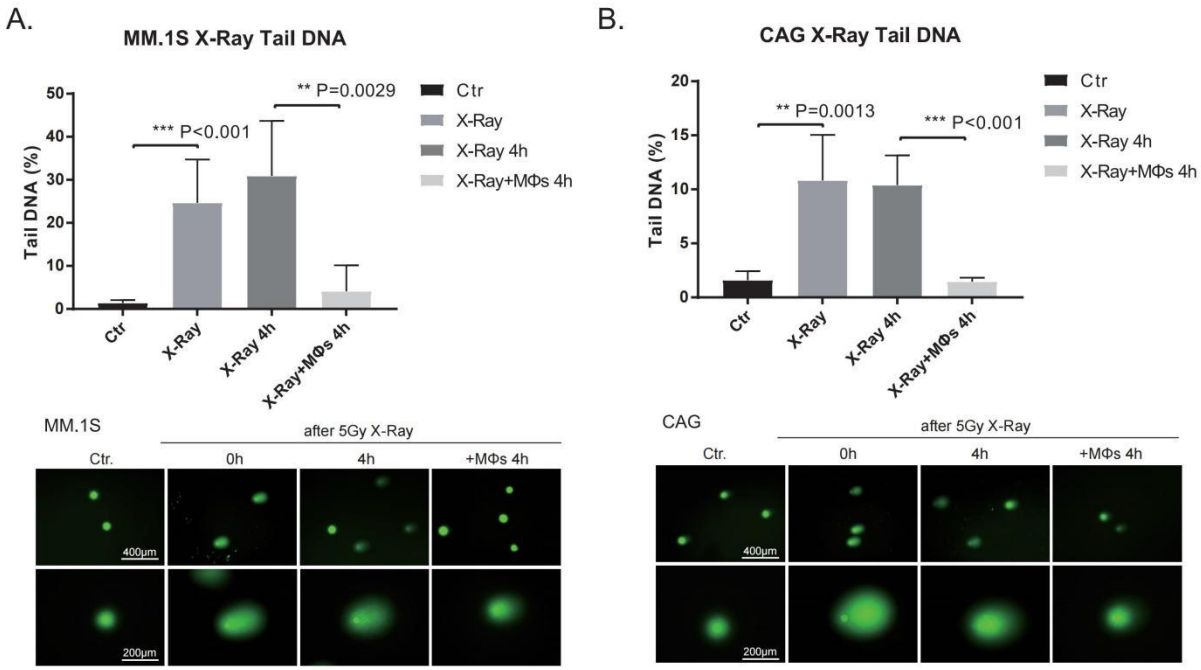

Figure S5, related to Figure 1. Comet assay of MM.1S (A) and CAG (B). Comet assay images showed damaged DNA in MM cells treated with X-ray irradiation for 5 Gy. CASP_1.2.3 software was applied to analyze the comet pictures and calculate the proportions of damaged DNA (unpaired two-tailed t-test). $0.01 \leq P < 0.05$, $0.001 \leq P < 0.01$, and $P < 0.001$ were regarded as *, **, and ***, respectively.

Figure S6

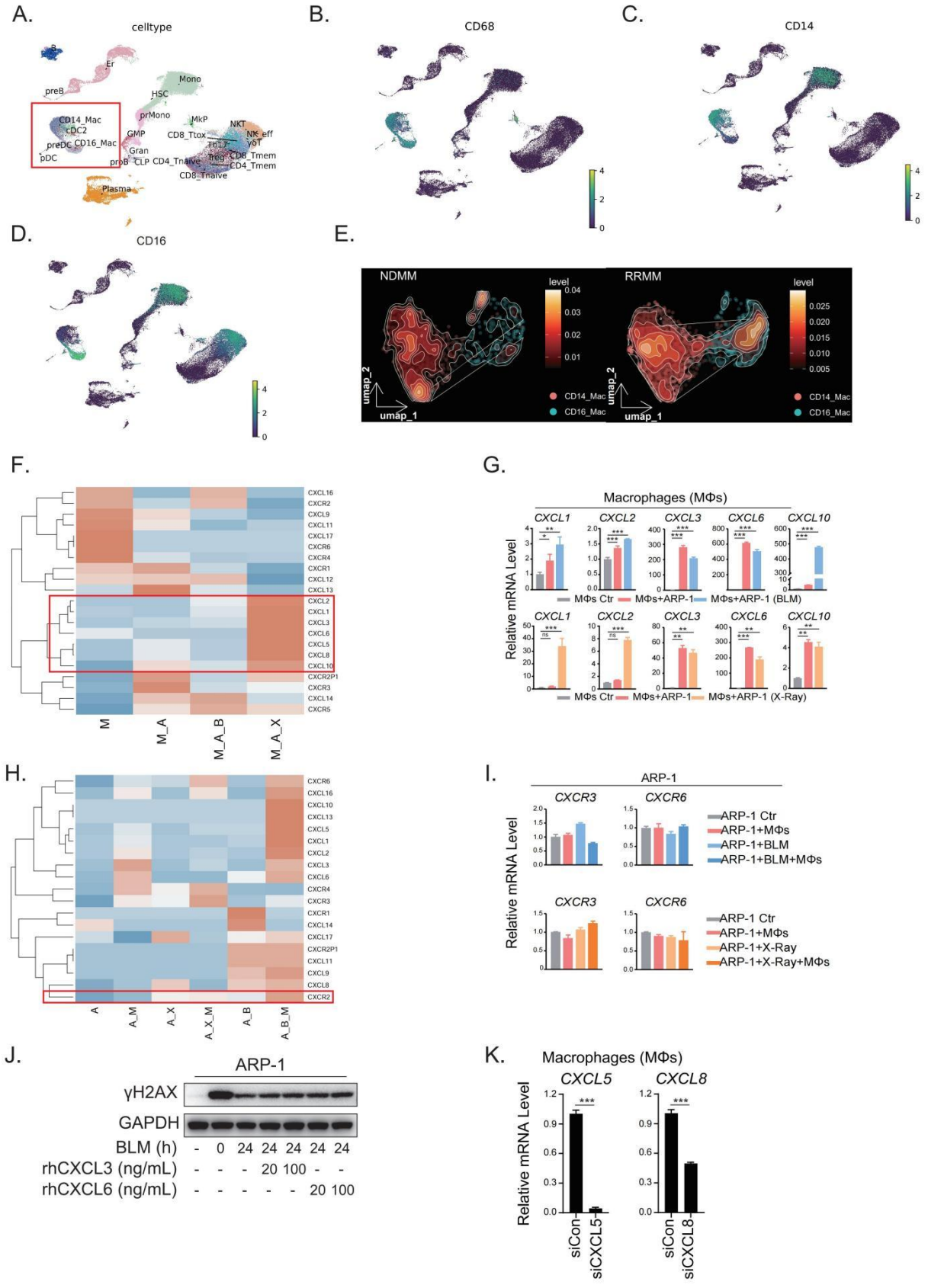

Figure S6, related to Figure 3. Single-cell RNA-seq and RNA-seq were adapted to screen the

pathways and subsequent experiments were conducted to verify them.

A-D. Single-cell RNA-seq sequencing of bone marrow cells from newly diagnosed MM (NDMM) and relapsed and refractory MM (RRMM) patients recognized the macrophages (A). Macrophages expressing CD68 (B), CD14 (C) and the other primarily expressing CD16 (D) are indicated.

E. Macrophages differs between NDMM and RRMM, which indicated the changes occurring among myeloma progression.

F. RNA-seq of multiple myeloma (MM) associated macrophages (MΦs) was done, and the groups are cultured alone (M), co-cultured with ARP-1 (M_A), co-cultured with ARP-1 treated with bleomycin (M_A_B) and X-Ray damage (M_A_X). The heatmap of RNA-seq showed that the expression of CXCLs in MΦs cocultured with ARP-1 increased.

G. RT-qPCR results showed the upregulation of CXCL1/2/3/6/10 transcription in MΦs by cocultured by ARP-1 cells (unpaired two-tailed t-test).

H. RNA-seq analysis of ARP-1 cells revealed increased expression of CXCR2 after DNA damage by X-Ray and bleomycin. The groups are ARP-1 (A), ARP-1 with MΦs (A_M), X-Ray treated ARP-1 alone (A_X) or with MΦs (A_X_M), and bleomycin treated ARP-1 alone (A_B) or with MΦs (A_B_M).

I. RT-qPCR showed the upregulation of CXCR3/6 expression in ARP-1 cells after DNA damage (unpaired two-tailed t-test).

J. Addition of CXCL3 or CXCL6 recombinant proteins to ARP-1 cells resulted in no effect on DNA repair of ARP-1 cells.

K. RT-PCR were conducted for validating the effect of siCXCL5/8.

Figure S7

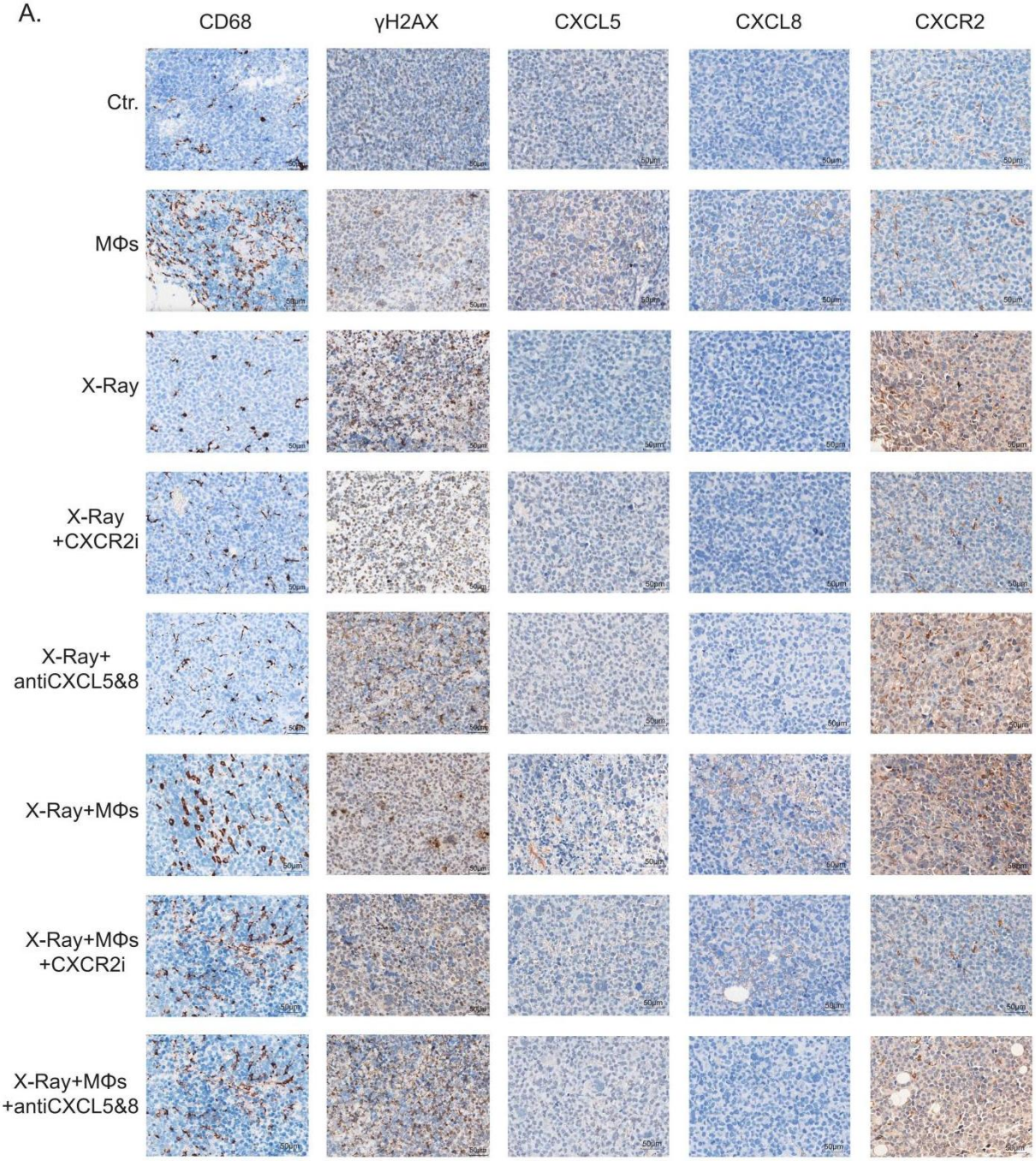

Figure S7, related to Figure 4. Immunohistochemistry of subcutaneous tumors in the NOD-SCID mice.

A. Immunohistochemical marked MΦs, CXCL5/8, CXCR2 and γH2AX. The results showed that the γH2AX in the X-Ray group was significantly higher than that in the control group, and MΦs injection reduced the γH2AX of MM cells. CXCR2 antagonist and CXCL5&8 neutralizing antibody weaken the promoting effect of MΦs on DNA repair in MM cells in vivo.

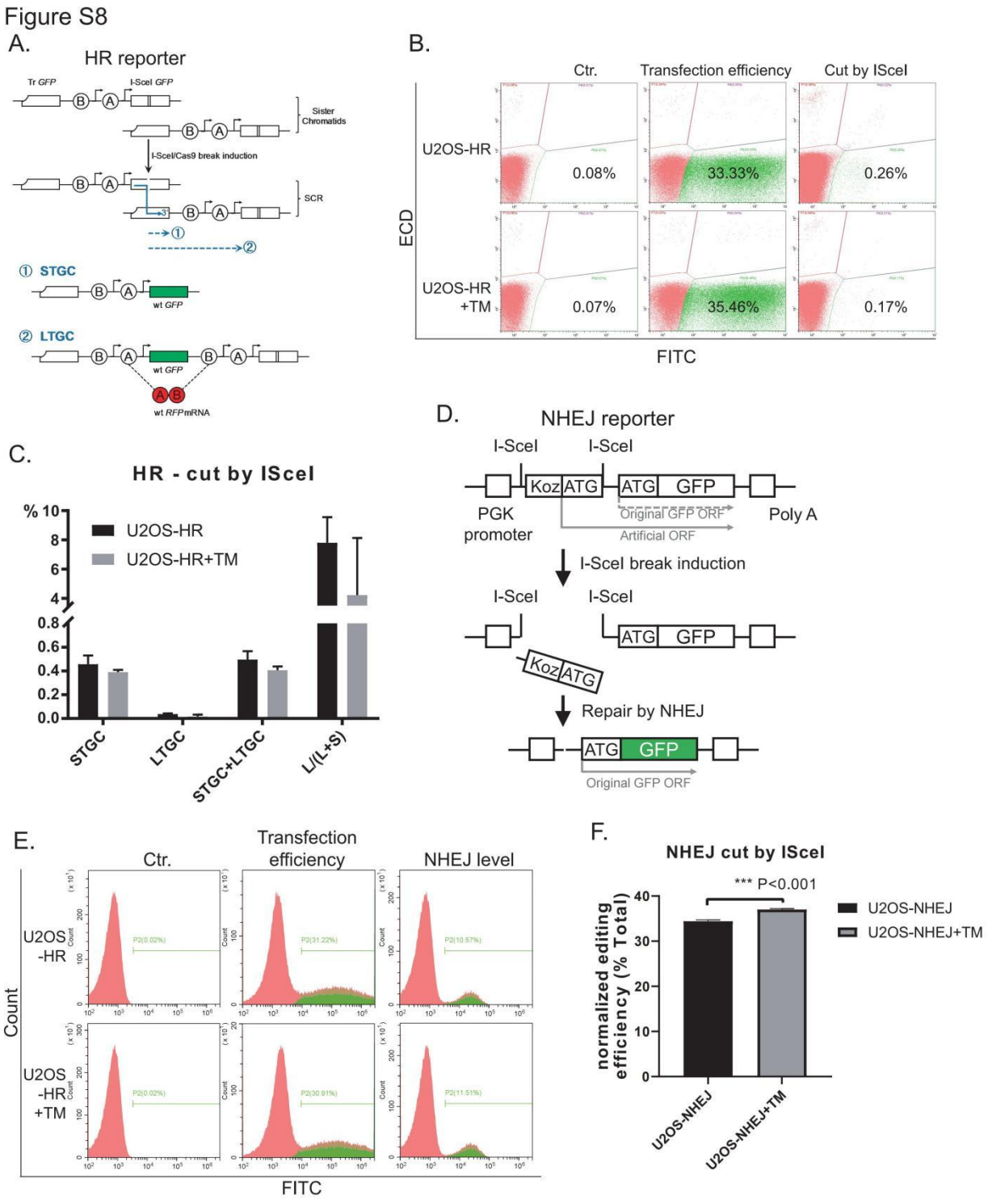

Figure S8, related to Figure 4. MΦs promote NHEJ rather than HR repair in MM cells in vitro.

A. Structure of the HR reporter. Repair of an I-SceI-induced DSB by HR between sister chromatids generates WT GFP. HR repair of I-SceI-induced DSBs in the HR reporter includes short-tract gene conversion (STGC), which generates $GFP^{+}RFP^{-}$ cells, and long-tract gene

conversion (LTGC), which generates GFP^+RFP^+ cells.[8, 9] Our research focused on the overall level of HR repair, i.e., the combined value of STGC and LTGC was corrected by the transfection efficiency of the I-SceI expression plasmid.

B. Flow cytometry was used to determine the transfection efficiency of the I-SceI plasmid by detecting GFP plasmid transfection efficiency.

C. MΦs showed no significant effect on the overall level of HR repair (STGC+LTGC) of U2OS cells.

D. Structure of the NHEJ reporter. 'Koz-ATG' denotes an artificial Kozak-ATG translation start site. ORF, open reading frame; PGK, phosphoglycerate kinase; PolyA, polyadenylation signal.

E. Flow cytometry was used to determine the transfection efficiency of the I-SceI plasmid by detecting GFP plasmid transfection efficiency.

F. Transwell-culture with the MΦs showed increased NHEJ repair of U2OS cells.

Figure S9

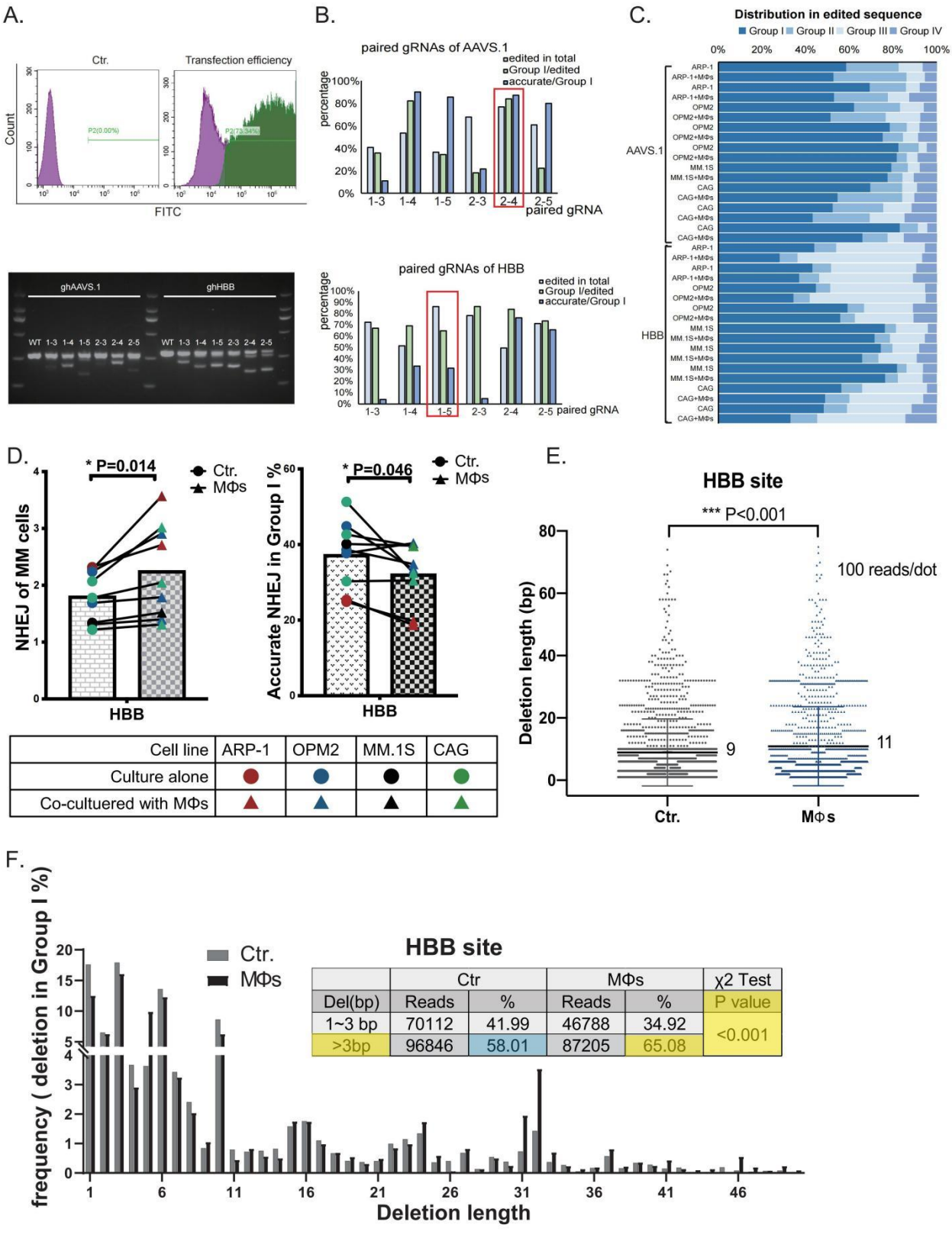

Figure S9, related to Figure 5. Selection of paired gRNAs and efficiency test for NHEJ test of MM

cells at the HBB site.

A. Flow cytometry was used to detect the transfection efficiency of the plasmids by detecting GFP plasmid transfection efficiency. PCR and gel electrophoresis were used to detect the cutoff efficiency of the paired SpCas9-sgRNAs. Efficient double cutting efficiency led to two significant binds.

B. Next Generation Sequencing (NGS) was used to detect the target sequences in AAVS.1 and HBB genes cut by the paired SpCas9-sgRNAs. A pair of gRNAs were screened for AAVS. 1 and HBB, respectively for the following experiments.

C. Groups I, II, III and IV in each MM cell experiment are shown.

D. Coculture with MΦs increased the efficiency of overall NHEJ (paired two-tailed t-test) at the HBB site. Coculture with MΦs reduced the frequency of accurate NHEJs in Group I (paired two-tailed t-test) at the HBB site.

E. The median length of Group I deletions with MΦs was 11 bp at the HBB site, longer than 9 bp at either site in MM cells without the MΦs coculture (Mann-Whitney test, $P < 0.001$).

F. Coculture with MΦs caused more frequent mutagenic NHEJ events with deletions of over 3 bp at the HBB site (G, 65.08% vs. 58.01% with or without MΦs; $\chi 2$ test, $P < 0.001$).

Figure S10

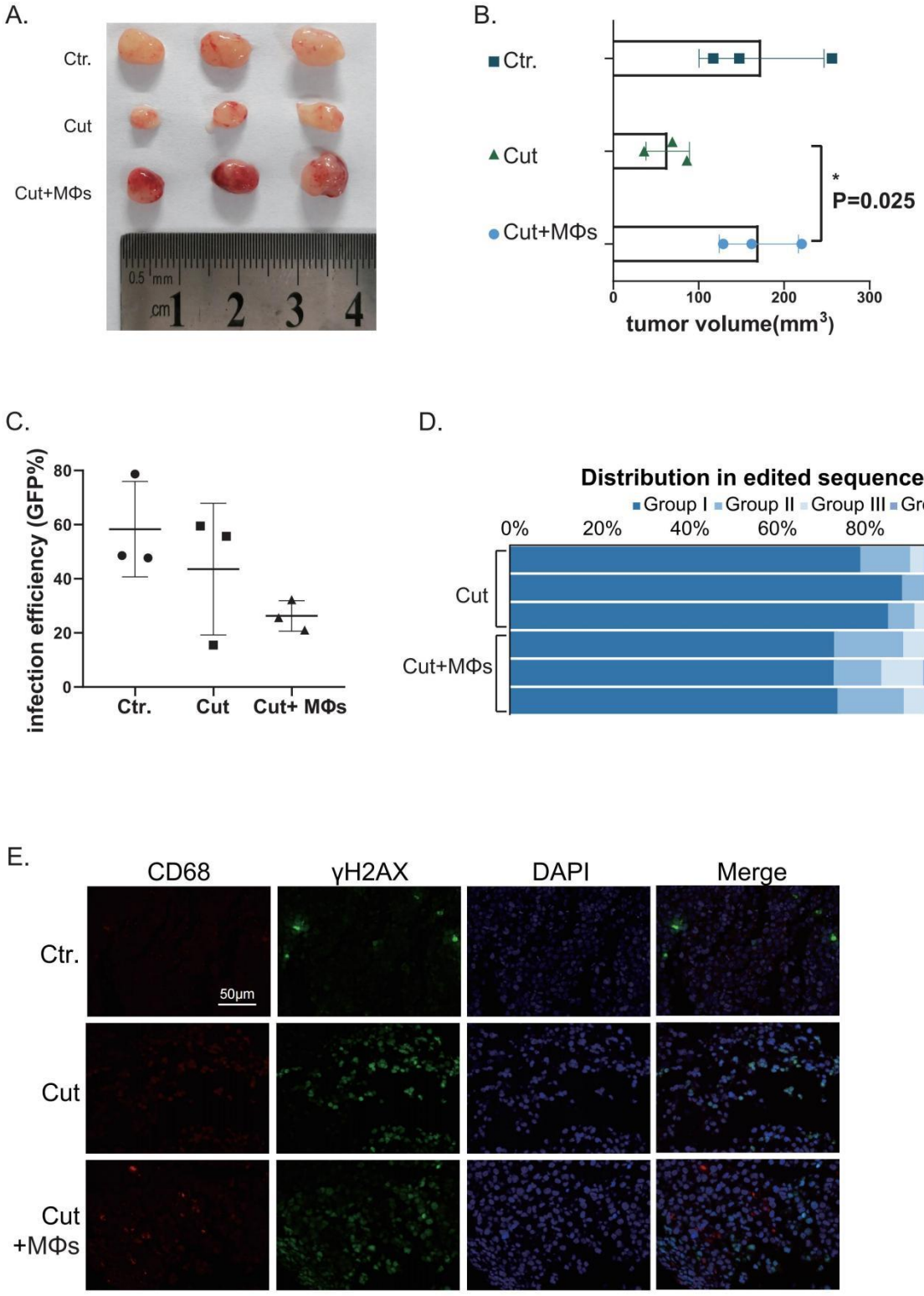

Figure S10, related to Figure 6. Supplementary figures for MΦs promoting mutagenic NHEJ in MM cells in vitro.

A. Tumors with MΦs injection or not.

B. The tumors in the MΦs group were larger than those in the gene-editing-only group (unpaired two-tailed t-test). The Volume=1/2 (length × width2).

C. Flow cytometry was applied to detect GFP expression to estimate the efficiency of virus infection.

D. Groups I, II, III and IV in the gene-editing-only (cut) and the MΦ (cut + MΦs) groups in each MM cell experiment are shown.

E. Immunofluorescence labeling showed that MΦs reduced DNA damage caused by paired Cas9-gRNAs' splicing, which meant compared with the cut group alone, the MΦs injection group showed a decrease in γH2AX.

Figure S11. The explanatory model

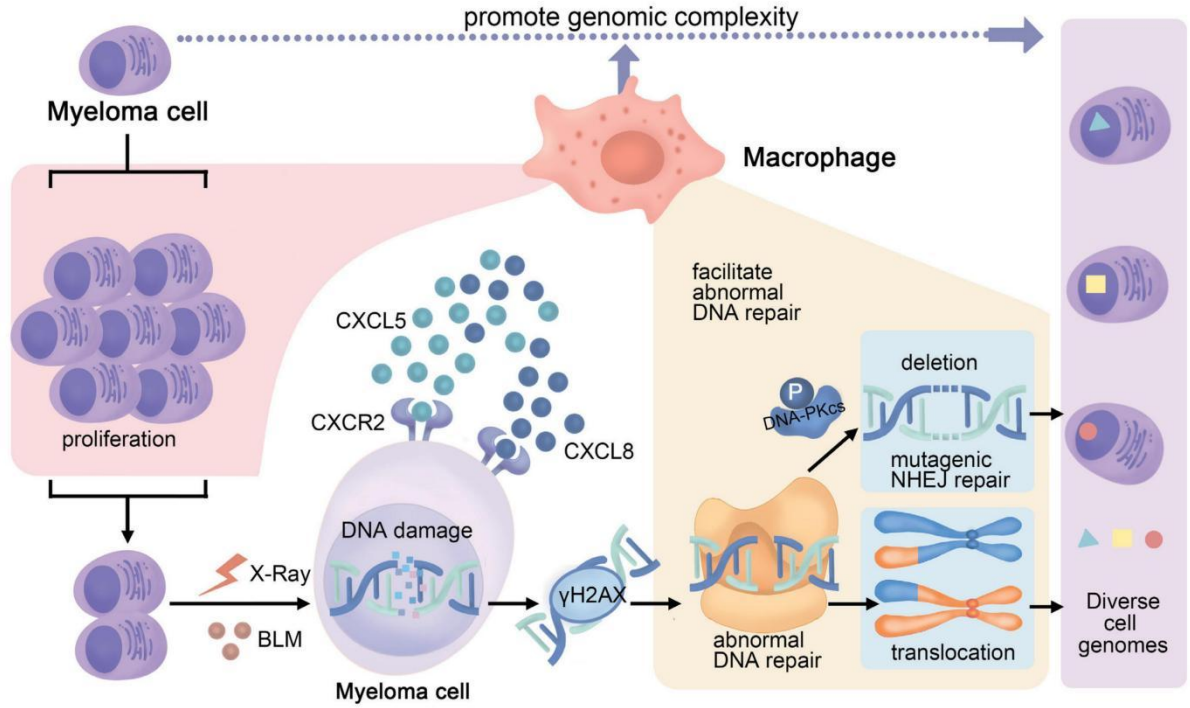

Figure S11. The explanatory model.

4) Supplementary Tables S1-S6

Table S1. Primers for RT-PCR

Target gene	Name	The sequence (5' to 3')
UBB	UBB-F	CGGCAAGACCATCACTCTGG
	UBB-R	AAAGAGTGCGGCCATCTTCC
ACTB	ACTB-F	GTTGTCGACGACGAGCG
	ACTB-R	GCACAGAGCCTCGCCTT
CXCL1	CXCL1-F	CCAGACCCGCCTGCTGAG
	CXCL1-R	CCACGGACGCTCCTGCTG
CXCL2	CXCL2-F	TGCAGGGAATTCACCTCAAG
	CXCL2-R	CTGGTCAGTTGGATTTGCCAT
CXCL3	CXCL3-F	CGCCCAAACCGAAGTCATAG
	CXCL3-R	GCTCCCCTTGTTCAGTATCTTTT
CXCL5	CXCL5-F	AGCTGCGTTGCGTTTGTTTAC
	CXCL5-R	TGGCGAACACTTGCAGATTAC
CXCL6	CXCL6-F	ACTATGAGCCTCCCGTCCAG
	CXCL6-R	GGGAACACCTGCAGTTTACCA
CXCL8	CXCL8-F	AGACAGCAGAGCACACAAGC
	CXCL8-R	ATGGTTCCTTCCGGTGGT
CXCL10	CXCL10-F	GTGGCATTCAAGGAGTACCTC
	CXCL10-R	TGATGGCCTTCGATTCTGGATT
CXCL16	CXCL16-F	GACATGCTTACTCGGGGATTG
	CXCL16-R	GGACAGTGATCCTACTGGGAG
CXCR2	CXCR2-F	CCTGTCTTACTTTTCCGAAGGAC
	CXCR2-R	TTGCTGTATTGTTGCCCATGT
CXCR3	CXCR3-F	CCACCTAGCTGTAGCAGACAC
	CXCR3-R	AGGGCTCCTGCGTAGAAGTT
CXCR6	CXCR6-F	GACTATGGGTTCAGCAGTTTCA
	CXCR6-R	GGCTCTGCAACTTATGGTAGAAG

Table S2. Annealing primers for paired gRNAs targeting AAVS1 and HBB sites

Target gene	Name	The sequence (5' to 3')
AAVS1	ghAAVS1-1-F	CACCGGTCCCCTCCACCCCACAGT
	ghAAVS1-1-R	AAACACTGTGGGGTGGAGGGGACC
	ghAAVS1-2 -F	CACCGGGGCCACTAGGGACAGGAT
	ghAAVS1-2 -R	AAACATCCTGTCCCTAGTGGCCCC
	ghAAVS1-3 -F	CACCGCTTCCTAGTCTCCTGATATT
	ghAAVS1-3 -R	AAACAATATCAGGAGACTAGGAAGC
	ghAAVS1-4 -F	CACCGAGACCCAATATCAGGAGACT
	ghAAVS1-4 -R	AAACAGTCTCCTGATATTGGGTCTC
	ghAAVS1-5 -F	CACCGTGTTAGGCAGATTCCTTATC
	ghAAVS1-5 -R	AAACGATAAGGAATCTGCCTAACAC
HBB	ghHBB-1- F	CACCGGGTATCAAGGTTACAAGAC
	ghHBB-1- R	AAACGTCTTGTAACCTTGATACCC
	ghHBB-2 -F	CACCGACCAATAGAAACTGGGCATG
	ghHBB-2 -R	AAACCATGCCCAGTTTCTATTGGTC
	ghHBB-3 -F	CACCGCACGTTCACCTTGCCCCACA
	ghHBB-3 -R	AAACTGTGGGGCAAGGTGAACGTGC
	ghHBB-4 -F	CACCGCATGGTGCATCTGACTCCTG
	ghHBB-4 -R	AAACCAGGAGTCAGATGCACCATGC
	ghHBB-5 -F	CACCGGTAACGGCAGACTTCTCCTC
	ghHBB-5 -R	AAACGAGGAGAAGTCTGCCGTTACC

Table S3. PCR primers for the AAVS1 and HBB sites

Target gene	Name	The sequence (5' to 3')
AAVS1	AAVS1-F	TGGGACCACCTTATATTCCC
	AAVS1-R	CATCGTAAGCAAACCTTAGA
HBB	HBB-F	GGGTGGGAAAATAGACCAAT
	HBB-R	CAGAGCCATCTATTGCTTAC
AAVS.1	ghAAVS1-F	CACCGGGGCCACTAGGGACAGGAT
	ghAAVS1-R	AAACATCCTGTCCCTAGTGGCCCC

Table S4. Annealing primers for gRNAs inducing chromosomal translocations

Target gene	Name	The sequence (5' to 3')
HBB	ghHBB-F	CACCGACCAATAGAAACTGGGCATG
	ghHBB-R	AAACCATGCCCAGTTTCTATTGGTC
IgH	ghIgH-F	CACCGGAGAACATACCAAGCCCCAC
	ghIgH-R	AAACGTGGGGCTTGGTATGTTCTCC
CCND1	ghCCND1-F	CACCGGTGGCGAGGTGGGACCGCGG
	ghCCND1-R	AAACCCGCGGTCCCACCTCGCCACC

Table S5. PCR primers for translocations

Target gene	Name	The sequence (5' to 3')
IgH-CCND1 der11 (for 400 bp)	PL-IgH-CCND1-11-F	TCTCCAAAGAGAAGCCACGT
	PL-IgH-CCND1-11-R	TCCACTAGAAGGGGAACTGG
IgH-CCND1 der14 (for 400 bp)	PL-IgH-CCND1-14-F	TCTGAGTCTGCAGTAAACCCCT
	PL-IgH-CCND1-14-R	CCGGGGAATCCTGAAGGTGTT
IgH-CCND1 der14 (for 250 bp)	PM-IgH-CCND1-14-F	AATCGCTTTGGAAGGCATGG
	PM-IgH-CCND1-14-R	CACTACCTGGCGTTCCAAGA
actin (for 250 bp)	P-actin-F	AAGACCTGTACGCCAACACA
	P-actin-R	AGTACTTGCGCTCAGGAGGA

Table S6. Cell types and marker genes for single cell analysis

Cell type	Abbreviation	Main marker gene(s)and features
Mature B-cell	B	MS4A1+/CD19+
CD14+ Macrophage	Mac_CD14	CD68+, CD14+
CD16+ Macrophage	Mac_CD16	CD68+, CD16+/FCGR3A+
CD4+ T-cell	T_CD4	CD3D+,CD3E+,CD4+
CD8+ T-cell	T_CD8	CD3D+,CD3E+,CD8A+
Conventional dendritic cell2	cDC2	CLEC10A+
Common lymphoid progenitor	CLP	IGLL1+,ADA+
Erythroblast	Er	AHSP+
Granulocyte-monocyte progenitor	GMP	ELANE+
Hematopoietic stem cell	HSC	AVP+
Megakaryocyte progenitor	MkP	PF4+
Monocyte	Mono	CD14+/CD11b+
NKdim effector cell	NK_eff	NKdim;GZMBhigh,PRF1high,CD16+/FCGR3Ahigh
NK T-cell	NKT	CD3D+,CD56/NCAM1dim,FCGR3Aim,KLRC2+
Plasmacytoid dendritic cell	pDC	CLEC4C+
Plasma cell	Plasma	CD138+,CD38+,MZB1+
Dendritic cell precursor	preDC	IGLL1+
Regulatory T-cell	Treg	CD3D+,CD40LG+,IL2RA+,FOXP3+
γδT-cell	γδT	CD3D*,CD3E*,TRDC+,TRGC1+